Gondwana Research 19 (2011) 788–799

Contents lists available at ScienceDirect

Gondwana Research

journal homepage: www.elsevier.com/locate/gr

The structure of the upper mantle beneath the Delamerian and Lachlan orogens from simultaneous inversion of multiple teleseismic datasets

N. Rawlinson [a,*], B.L.N. Kennett [a], E. Vanacore [a], R.A. Glen [b], S. Fishwick [c]

[a] Research School of Earth Sciences, The Australian National University, Canberra ACT 0200, Australia
[b] Geological Survey of New South Wales, Department of Industry and Investment, PO Box 344 Hunter Regional Mail Centre NSW 2310, Australia
[c] Department of Geology, University of Leicester, Leicester LE1 7RH, UK

ARTICLE INFO

Article history:
Received 29 January 2010
Received in revised form 5 November 2010
Accepted 9 November 2010
Available online 23 November 2010

Keywords:
Seismic tomography
Lithosphere
Australia
Lachlan Orogen
Delamerian Orogen

ABSTRACT

Distant earthquake data recorded by seven sub-arrays of the ongoing WOMBAT rolling seismic array deployment in southeast Australia are combined for the first time to constrain 3-D variations in upper mantle P-wavespeed via teleseismic tomography. The seven arrays comprise a total of 276 short period recorders spaced at intervals of approximately 50 km, thus allowing unprecedented resolution of the upper mantle over a large region. In the mantle lithosphere immediately below the crust (~50 km depth), dominant variations in velocity tend to strike east–west, and share little resemblance to Palaeozoic boundaries in the shallow crust inferred from surface geology and potential field data. A broad region of elevated wavespeed beneath northern Victoria may represent the signature of underplated igneous rocks associated with detachment faulting during the break-up of Australia and Antarctica. A distinct low velocity anomaly in southern Victoria appears to correlate well with the Quaternary Newer Volcanic Provinces. Towards the base of the mantle lithosphere, the dominant structural trend becomes north–south, and five distinct velocity zones become apparent. Of particular note is a transition from higher wavespeed in the west to lower wavespeed in the east beneath the Stawell Zone, implying that the Proterozoic lithosphere of the Delamerian Orogen protrudes eastward beneath the Western subprovince of the Lachlan Orogen. This transition zone extends northwards from southern Victoria into central New South Wales (the northward limit of the arrays), and is one of the dominant features of the model. Further east, there is a transition from lower to higher wavespeeds in the vicinity of the boundary between the Western and Central subprovinces of the Lachlan Orogen, which has several plausible explanations, including the existence of a Proterozoic continental fragment beneath the Wagga–Omeo Zone. The presence of elevated wavespeeds beneath the Melbourne Zone in Victoria, although not well constrained due to limited data coverage, provides some support to the Selwyn Block model, which proposes a northward extension beneath Bass Strait of the Proterozoic core of Tasmania.

1. Introduction

The Tasman Orogen or Tasmanides (Foster and Gray, 2000; Glen, 2005; Foster et al., 2009) of eastern Australia largely consists of a series of accretionary orogens that formed outboard of the Pacific margin of eastern Gondwana from the Middle Cambrian through to the Middle Triassic (Glen, 2005). Occupying approximately one-third of present day Australia, the Tasmanides incorporate five orogenic belts, including the Delamerian and Lachlan orogens in the south (see Fig. 1), the Thomson and North Queensland orogens in the north, and the New England Orogen in the east. The Delamerian Orogen, which incorporates the Adelaide Fold Belt in South Australia, extends southward from the mainland into Tasmania, where it is often referred to as the Tyennan Orogen (Berry et al., 2008). It comprises Precambrian and Early Cambrian rock sequences that were subject to contractional orogenesis along the eastern margin of Gondwana between about 514 Ma and 490 Ma (Foden et al., 2006). This was followed in the Late Cambrian by the formation of the Lachlan Orogen to the east, which continued through to the Early Carboniferous.

Large tracts of the Lachlan and Delamerian orogens that would otherwise be exposed at the surface are masked by the presence of younger Mesozoic–Cainozoic sedimentary and volcanic cover sequences. For example, the intra-cratonic Murray Basin overlies much of the Delamerian Orogen and a large portion of the Western Subprovince of the Lachlan Orogen (see Fig. 1) and obscures the boundary between them. The resulting lack of outcrop has helped foster a variety of plausible models that seek to explain the formation of the southern Tasmanides. For instance, Foster and Gray (2000), Spaggiari et al. (2003, 2004) favour an accretionary oceanic system involving multiple Ordovician–Silurian coeval subduction zones inboard of the plate boundary, whereas VandenBerg (1999), Taylor and Cayley (2000), Willman et al. (2002), Glen (2005) and Glen et al.

* Corresponding author. Tel.: +61 2 6125 5512; fax: +61 2 6257 2737.
E-mail address: nick@rses.anu.edu.au (N. Rawlinson).

1342-937X/$ – see front matter
doi:10.1016/j.gr.2010.11.001

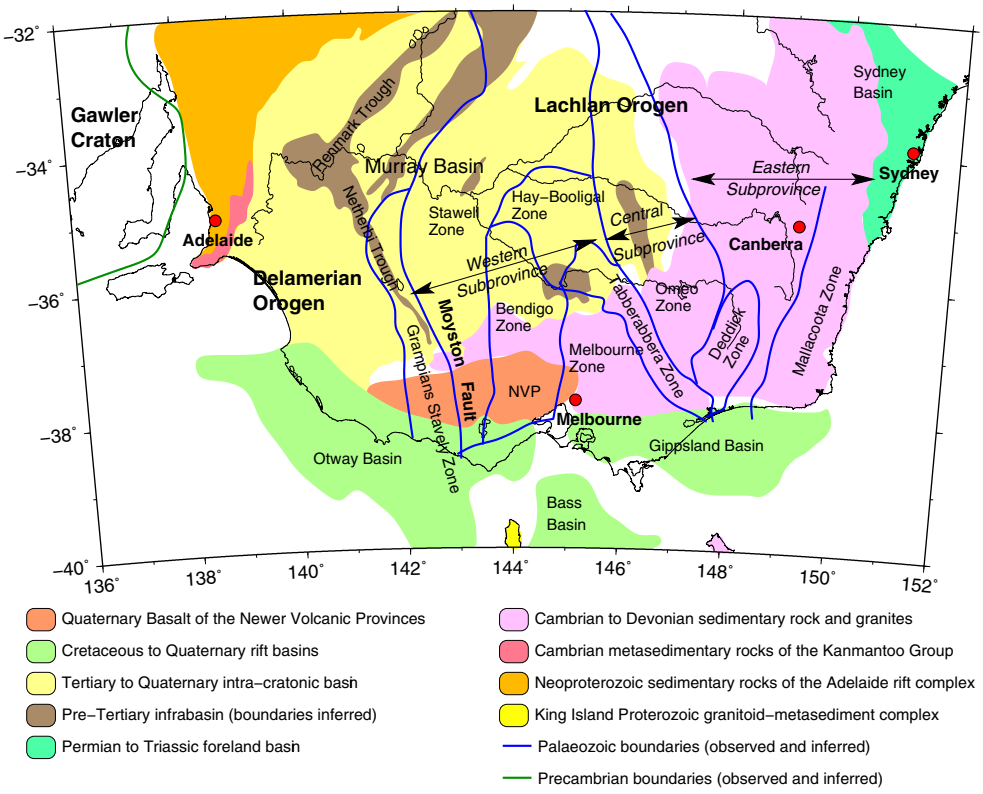

Fig. 1. Simplified map showing broad scale surface geology and Palaeozoic tectonic boundaries in southeast Australia. The three subprovinces of the Lachlan Orogen are also marked.

(2009) argue against this scenario and for the involvement of orogen-parallel strike-slip tectonics. Furthermore, there is no clear consensus regarding the origin of the underlying lithosphere, which may range from purely oceanic to mixed oceanic and continental (Rutland, 1976; Glen, 2005). One possible source of continental material comes from the break-up of the supercontinent Rodinia, which may have set adrift a number of Precambrian continental ribbons or fragments which were subsequently incorporated within the convergent accretionary system responsible for the formation of the Lachlan Orogen (Cayley et al., 2002; Direen and Crawford, 2003).

The location of the boundary between the Delamerian and Lachlan orogens at the surface has proven difficult to resolve, with a number of different possibilities put forward by various authors over the last several decades (e.g. VandenBerg, 1978; Baillie, 1985; Foster and Gleadow, 1992). More recently, the Moyston Fault, which marks the boundary between the Stawell Zone and Grampians–Stavely Zone, has become the preferred location of the transition between the two orogens (Cayley and Taylor, 1998; VandenBerg, 1999; Cayley et al., 2002; Korsch et al., 2002). Korsch et al. (2002) infer the presence of the Moyston Fault in a deep seismic reflection transect from western Victoria as an east dipping boundary that extends in depth to at least 15 km. Due to the presence of reflections in the hanging wall that resemble ramp anticlines, they interpret the fault to be a thrust, with the Lachlan Orogen thrust westward over the upper part of the Delamerian Orogen. Miller et al. (2005) propose a new tectonic model that describes the evolution of the Delamerian and Lachlan orogens, and explains why the boundary between the two is hard to resolve. They use $^{40}Ar/^{39}Ar$ data to identify a Cambrian metamorphic belt immediately east of the Moyston Fault, and infer the presence of a Palaeozoic continental fragment underlying the Grampians–Stavely Zone. This model allows for a subduction zone that dips west towards the Gondwana supercontinent, but at the same time gives rise to an east dipping Moyston Fault via slab rollback and subsequent shortening. In this scenario, a reworked orogenic zone that spans the Moyston Fault and contains elements of both the Delamerian and Lachlan orogens is present.

In this study, high resolution teleseismic tomography using new passive seismic data from WOMBAT, a large program of rolling array deployments in southeast Australia (see Fig. 2), is carried out to image the upper mantle structure beneath the Delamerian and Lachlan orogens. Arrival time residual information from seven separate deployments comprising a total of 276 stations is combined to constrain 3-D P-wave velocity variations beneath Victoria, New South Wales, and southeastern South Australia. Although the inversion of such a large dataset is expected to reveal a wealth of information on the seismic structure of this region, our focus will be on the nature of the lithospheric boundary between the Delamerian and Lachlan orogens, and the extent to which Precambrian lithosphere extends from the Delamerian Orogen eastward beneath the Western Subprovince of the Lachlan Orogen (Graeber et al., 2002; Rawlinson et al., 2006a).

The idea of a rolling passive seismic array in southeast Australia began with the three stage MALT project (incorporating LF98, MB99 and AF00) in 1998, and slowly began to unfold into a large ongoing program called WOMBAT which has a long term goal of spanning much of eastern Australia with seismic stations at approximately 50 km intervals. To date, over 500 stations have been deployed, with two new arrays of at least 40 stations each scheduled for deployment in the next two years. WOMBAT is the largest project of its type in the southern hemisphere, and promises to deliver a sizable volume of passive seismic data that can be used for a variety of purposes, including body wave tomography, ambient noise surface wave tomography, crustal receiver functions and array studies of mantle discontinuities and core structure.

To date, most research carried out with WOMBAT data has involved 3-D teleseismic tomography using a single array — for example, LF98 (Graeber et al., 2002), AF00 (Clifford et al., 2008), TIGGER (Rawlinson et al., 2006b), SEAL (Rawlinson et al., 2006a) and EVA (Rawlinson and Kennett, 2008). While these studies have produced a variety of interesting results, the use of relative arrival time residual information makes it difficult to suture together

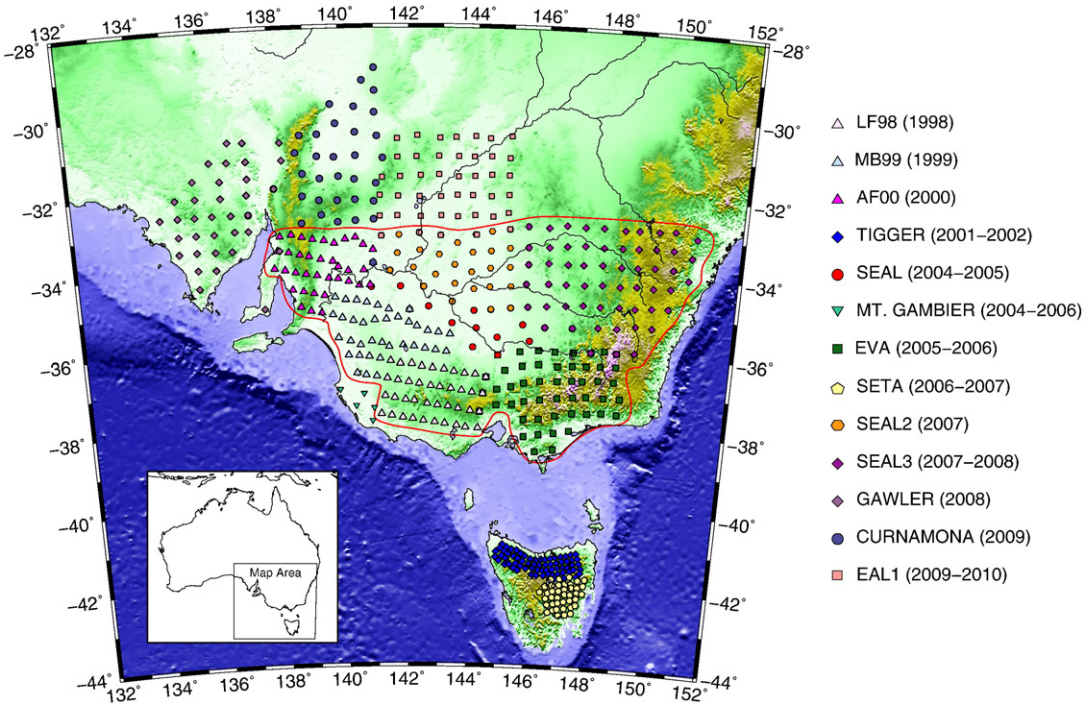

Fig. 2. Distribution of WOMBAT seismic stations in southeast Australia as at January 2010. In most cases, the sub-arrays are deployed sequentially, although there is occasionally some overlap. The red line encloses the seven sub-arrays used in the current study.

independently derived models from adjacent arrays. Thus, there is much to be gained by performing a joint inversion of all available teleseismic data for a single, unified, upper mantle model of P-wave velocity anomalies.

2. Data and method

The dataset used in this study is derived from distant earthquake records from seven WOMBAT arrays (outlined in red in Fig. 2). In each case, global catalogues are used to identify events that are likely to yield signals with good signal-to-noise ratio; this includes all earthquakes of magnitude Mw>6.0, any earthquake of Mw>5.0 within an approximately 100° radius, and an even lower threshold of Mw>4.5 for events from the south and west in order to optimise azimuthal coverage. A variety of global body wave types are targeted for extraction, including direct P, pP, PcP, ScP, PP and PKiKP, all of which produce sub-vertical ray paths beneath the receivers that are required for teleseismic tomography. The use of core reflection phases means that in some cases, earthquakes closer than the typical teleseismic threshold of ~27° can be included. All traces are subject to preliminary alignment using the *ak*135 global reference model of Kennett et al. (1995). The adaptive stacking technique of Rawlinson and Kennett (2004) is then used to align the traces of each phase recorded from a single earthquake in order to obtain relative arrival time residuals, which reflect lateral variations in wavespeed beneath the receiver array. The adaptive stacking technique automatically produces uncertainty estimates for each residual, thereby allowing for an automated system of picking arrivals. However, we also use manual inspection of trace stacks to ensure good picking quality. An example of a PKiKP (inner core reflection) phase recorded by SEAL2 is shown in Fig. 3; the good signal-to-noise ratio is typical of stations deployed in relatively remote parts of Australia that are largely free from ocean noise.

The typical number of earthquakes that produce usable data ranges between 100 and 200 for the seven arrays outlined in red in Fig. 2. Fig. 4 shows the distribution of all events used to constrain the teleseismic tomography model described in the next section. An obvious concern with this distribution is that it has a very strong azimuthal variation, with many events located in the north and east and relatively few located in the south and west. This unevenness will produce undesirable artefacts in the tomographic results by way of smearing out of anomalies along dominant ray path directions. In order to help mitigate this effect, we bin the data into 5°×5° cells, which results in a more even distribution of pseudo-sources. An added benefit of this process is the reduced computation time due to fewer overall paths. Tests made using 2.5°×2.5° bins produced essentially the same results but required additional computation time. The total number of paths available for tomographic imaging following all data processing procedures described previously is 19,922.

The relative arrival time residuals are mapped as 3-D perturbations in P-wavespeed from a 1-D (depth dependent) reference model using the teleseismic tomography method of Rawlinson et al. (2006b) and Rawlinson and Kennett (2008). A grid based eikonal solver known as the Fast Marching Method or FMM (Popovici and Sethian, 2002; Rawlinson and Sambridge, 2004a,b) is used to solve the forward problem of predicting source–receiver traveltimes, and a subspace inversion method (Kennett et al., 1988) is used to solve the inverse problem of varying the value of velocity nodes in order to satisfy data observations. The method is applied iteratively in order to address the non-linear nature of the inverse problem. Explicit damping and smoothing regularisation is used to prevent the recovered anomalies from becoming unreasonably large or complex.

A central assumption of teleseismic tomography is that relative arrival time residual patterns are largely unaffected by lateral variations in structure outside a local model volume positioned immediately below the array (Aki et al., 1977; Humphreys and Clayton, 1990; Graeber et al., 2002; Rawlinson and Kennett, 2008).

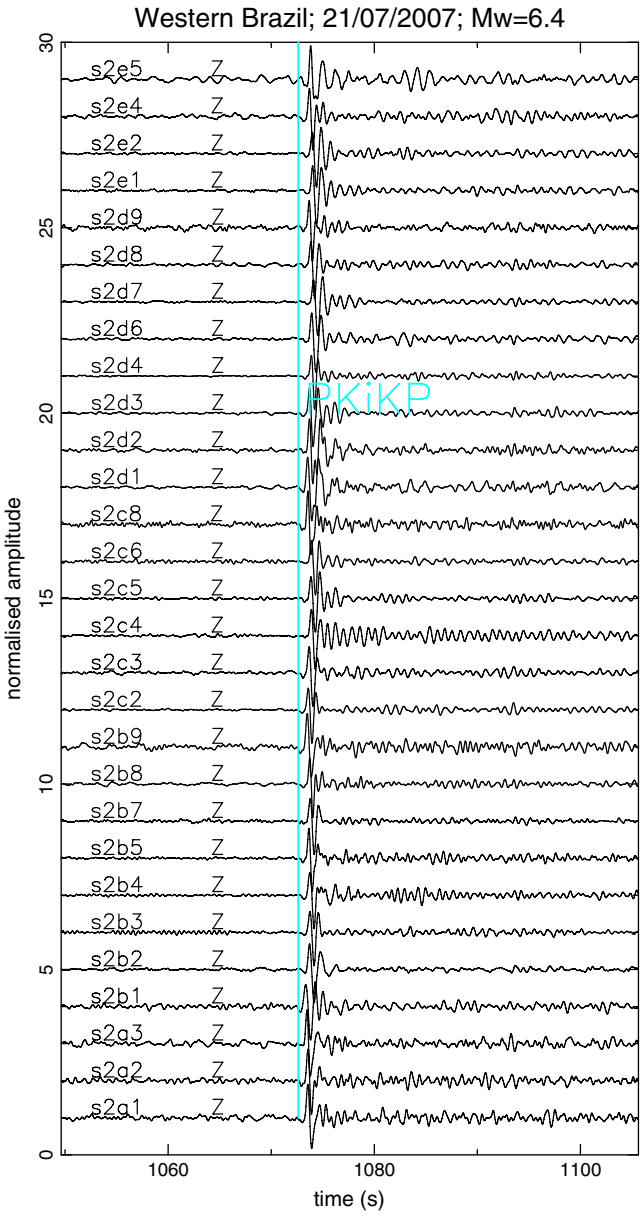

Fig. 3. Example of a very clear PKiKP phase recorded by the SEAL2 array. Note the coherence between the arriving signal at each station; this is exploited by the adaptive stacking routine to obtain precise relative arrival times. The coloured line indicates predictions from the global reference model *ak*135, to which all traces have been aligned.

Consequently, errors in source location and lateral variations in structure beneath the 3-D model are likely to manifest as artifacts in the tomographic results. However, these effects are likely relatively small compared to the potential for unresolved near-surface structure to affect relative arrival times and hence the solution model. One approach to minimising this problem is to use an accurate *a priori* crustal model to either correct traveltime residuals prior to inversion, or to constrain near-surface structure during the inversion (e.g. Waldhauser et al., 2002; Lippitsch et al., 2003; Martin et al., 2005; Lei and Zhao, 2007). A simple and popular alternative is to instead invert for station terms (Frederiksen et al., 1998; Graeber et al., 2002) which attempt to "absorb" near-surface contributions to arrival time residuals, but there is a trade-off between station terms and velocity structure that is difficult to resolve. In this case, no laterally heterogeneous prior model exists, so we

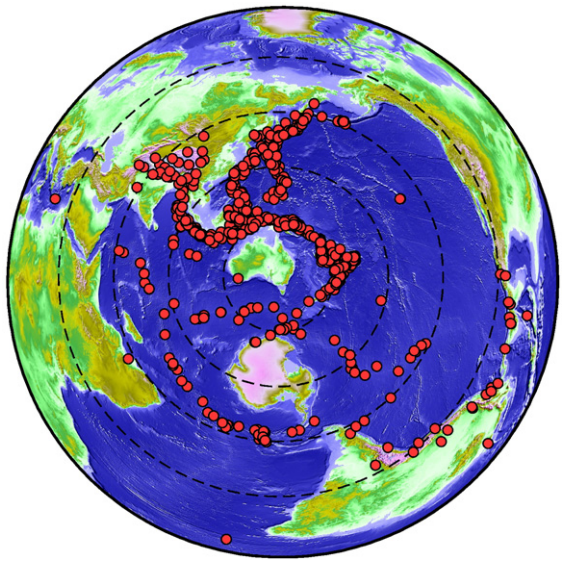

Fig. 4. Distribution of usable teleseismic events recorded by all seven arrays outlined in red in Fig. 2.

instead invert for station terms. Rawlinson and Kennett, 2008 show that the differences between the two methods for station spacings of about 50 km tend to be small below depths of approximately 70 km.

3. Results

3.1. Resolution tests

In general, inverse problems may be overdetermined, mixed-determined or underdetermined (Menke, 1989). Most seismic tomography problems fall within the latter two categories, meaning that many different solutions are capable of satisfying the data to the same extent. Consequently, regularisation is often imposed in an attempt to target solutions that are seen to be physically reasonable, usually in a qualitative sense (Rawlinson and Sambridge, 2003). In this case, damping and smoothing are imposed in order to find a solution that is not largely perturbed from the initial or starting model, and exhibits lateral heterogeneity only where required by the data. Thus, parsimony is favoured over complexity, which means that certain classes of structure will be favoured in the reconstruction. A standard approach for analysing solution non-uniqueness in seismic tomography is to perform a synthetic reconstruction test in which the forward problem is solved for some given model in order to produce a synthetic dataset, which has identical sources, receivers and phase types as the observational dataset. The synthetic dataset is then inverted using the same regularisation parameters in an attempt to reconstruct the input model; the differences between the input and output model provides an indication of the robustness of the solution (Rawlinson et al., 2010).

Here, we use a simple checkerboard test to analyse the resolving power of the dataset. The initial model used in the reconstruction consists of a laterally homogeneous P-wave model that conforms with *ak*135 at mantle depths, and a 1-D model of the Lachlan Orogen obtained from refraction data (Collins, 1991) at crustal depths. The input model comprises an alternating pattern of positive and negative anomalies – superimposed on the initial model – of a single scale length in all three dimensions, thus making comparison with the reconstructed output model a relatively simple task. The synthetic dataset is obtained by applying FMM in the presence of the checkerboard model, and adding Gaussian noise with a standard deviation of 50 ms in order to simulate the noise content of real data.

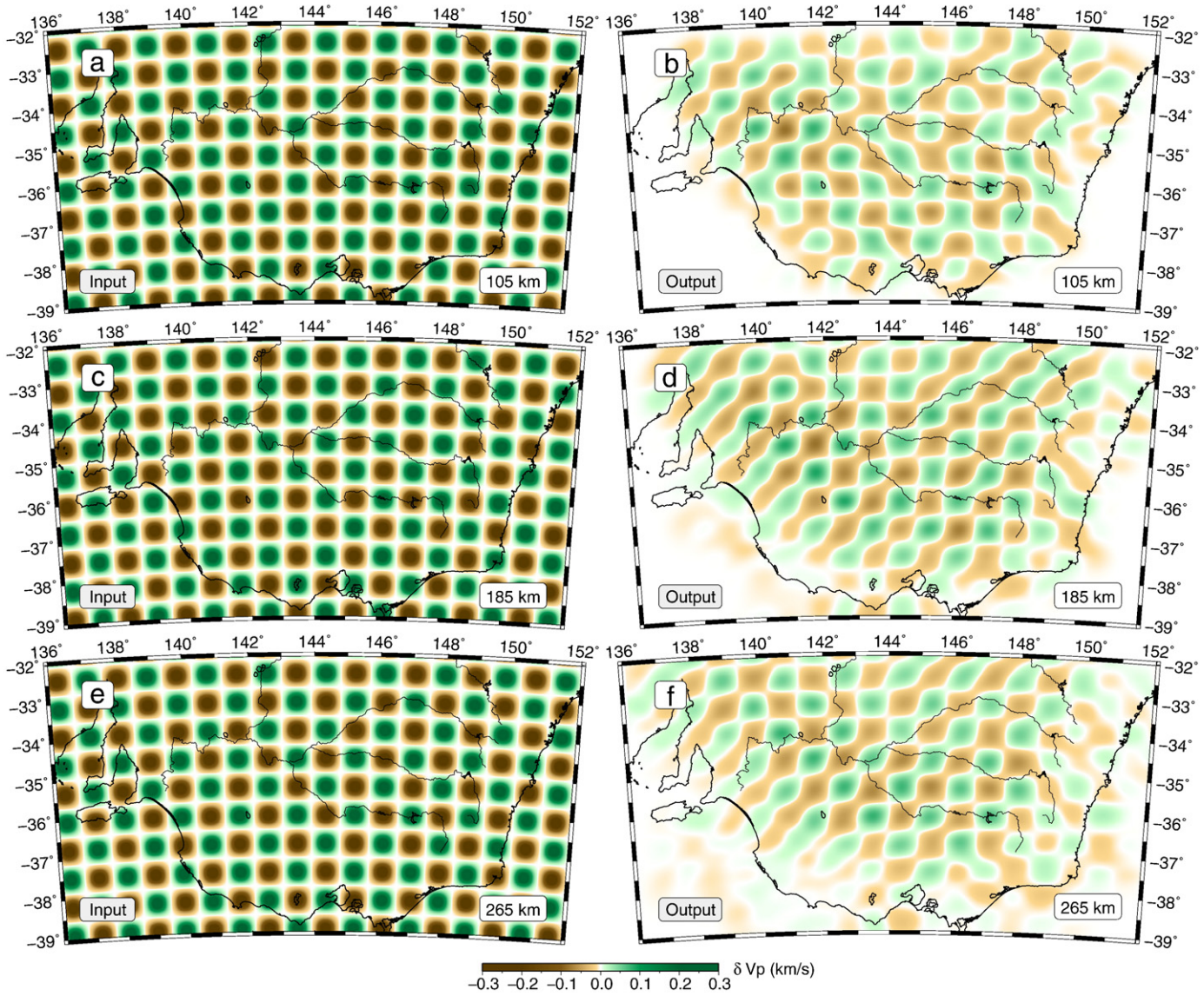

Fig. 5. Synthetic checkerboard resolution tests for the WOMBAT teleseismic dataset. The input models are shown on the left, and the output (or reconstructed) models are shown on the right, for a series of three depth sections.

The 3-D model volume spans 10.4° in longitude, 18.5° in latitude and 340 km in depth. Cubic B-spline functions are used to describe the smoothly varying velocity continuum, which is controlled by a regular velocity grid with a node spacing of approximately 20 km in all three dimensions. In total, there are 103,700 velocity nodes, which together with the station terms, constitute the unknowns in the inversion.

Figs. 5 and 6 show the results of the checkerboard resolution test after six iterations of the inversion method (with traveltimes and Fréchet derivatives updated after each iteration) in horizontal and vertical sections respectively. In general, the pattern of anomalies is well reconstructed, although there is evidence of sub-vertical smearing of rays near the edges of the model (see Fig. 6f in particular). Another phenomenon that can be easily observed is that the amplitude of anomalies in the reconstructed or output model generally underestimates that of the input model. This is a typical consequence of damping and smoothing regularisation, and means that while the pattern of recovered anomalies is generally quite well constrained, the amplitudes tend to be conservative. It is also noteworthy that the choice of colour scale influences the representation of velocity structure. Here, we use a standard two-tone colour scale which changes colour at zero perturbation. Thus, a smooth variation in wavespeed which crosses this value can give the appearance of a distinct boundary, when in fact one may not exist. Hence, our preference to use “transition” rather than “boundary” to describe apparently sharp changes in wavespeed.

Although use of checkerboard resolution tests is ubiquitous in the published literature (e.g. Hearn and Clayton, 1986; Glahn and Granet, 1993; Graeber and Asch, 1999; Rawlinson et al., 2006b), they have a number of limitations which mean that they are not viewed as a comprehensive test of solution robustness (Lévêque et al., 1993, for more details). In general, it is advisable to run a series of synthetic reconstruction tests in order to explore phenomena like the dependence of path geometry on velocity heterogeneity, and the predisposition of the path coverage to favour the reconstruction of certain classes of structure. We do not perform any additional tests here, but instead cite the papers of Rawlinson et al. (2006b) and Rawlinson and Kennett (2008), which present teleseismic tomography using the TIGGER and EVA datasets respectively. In both cases, multiple synthetic reconstruction tests are performed using a source distribution that is largely mimicked by all seven datasets used in this study.

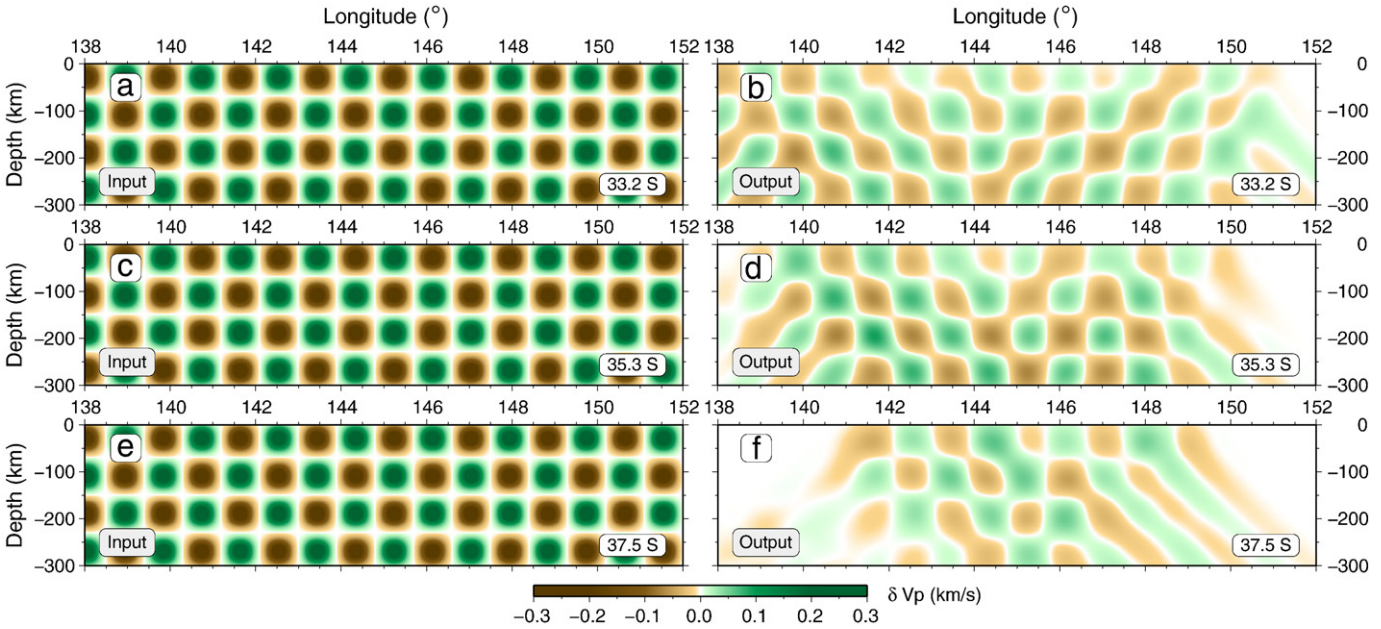

Fig. 6. Same as Fig. 5, but now showing E–W cross-sections.

3.2. On the use of relative arrival time residuals

The use of relative arrival time residuals to constrain structure has a number of advantages and drawbacks. One advantage is that cross-correlation type schemes can be used to accurately obtain the relative onset times of a phase at all simultaneously recording stations. Removal of the mean on a source-by-source basis means that origin time uncertainty (which can be much larger than the actual residuals) is no longer a factor, and traveltime contributions from large scale variations in mantle structure beneath the model region are suppressed. On the other hand, the velocity anomalies that are recovered are only meaningful in a relative sense (Priestley and Tilmann, 2009). This last factor means that the joining of datasets from adjacent arrays that are sequentially deployed is not straightforward. In the extreme case, it is possible for the same anomaly to be illuminated as a positive velocity perturbation by one array, and a negative velocity perturbation by another; for example if the velocity field is dominated by a strong horizontal velocity gradient. As a result it may not be appropriate to compare models obtained by separately inverting adjacent datasets.

In this study, all datasets are simultaneously inverted, and the use of "tie" stations (i.e. stations left behind to continue recording while the array is moved and installed at another location) between adjacent arrays helps to join the datasets together. Apart from not recovering absolute velocities, the main limitation that arises from the joining of relative arrival time datasets is the difficulty of resolving long wavelength features larger in size than the horizontal dimensions of the sub-arrays.

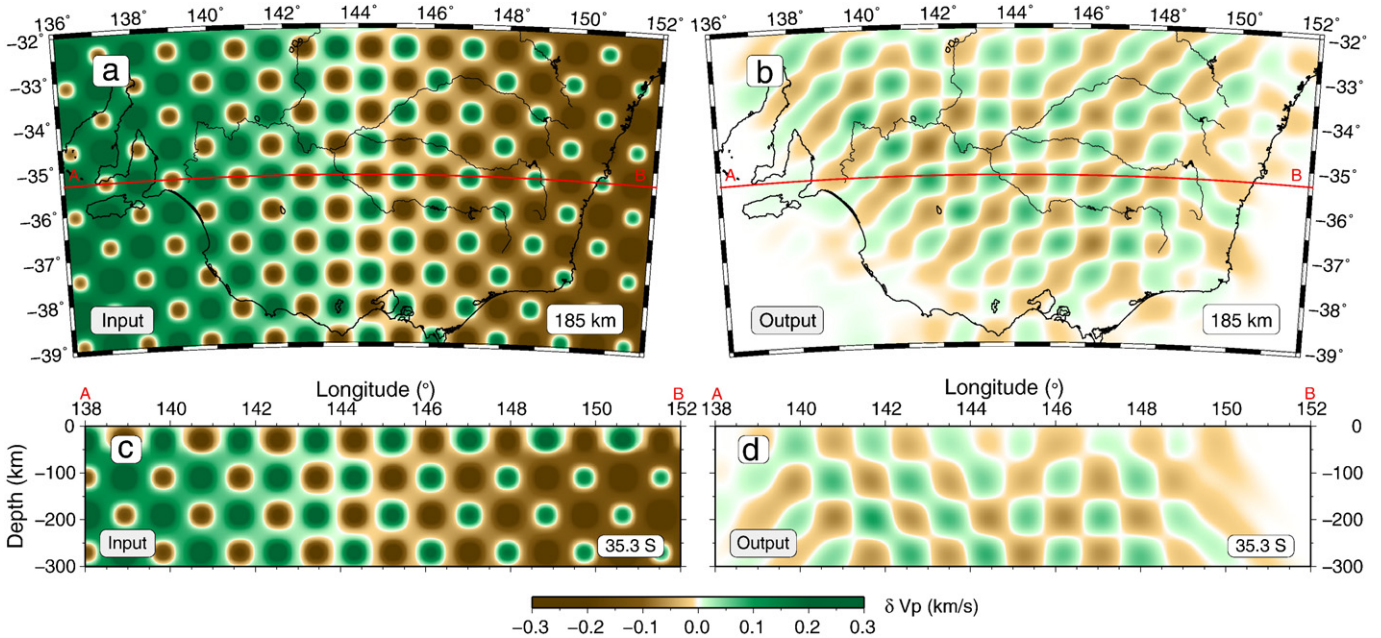

Fig. 7. Results of a synthetic checkerboard test identical to that performed in Figs. 5 and 6, except that now a horizontal velocity gradient oriented in the latitudinal direction is superimposed. cf. Figs. 5c and d and 6c and d.

In order to demonstrate this effect, we perform a checkerboard resolution test using exactly the same parameters as the test shown in Figs. 5 and 6, except that now a constant velocity gradient is superimposed on the mantle region of the synthetic model. The horizontal velocity gradient is oriented in the longitudinal direction, and results in a change in the background velocity from +0.2 km/s at the western edge of the model, and −0.2 km/s at the eastern edge. Fig. 7 shows a comparison between the input and output model at 185 km depth, and also along a cross-section at 35.3° south. Clearly, the horizontal velocity gradient is absent from the reconstruction, but the smaller-wavelength checkerboard is recovered in almost identical fashion to Figs. 5 and 6. An additional check on the validity of the procedure is that a comparison between the model derived in the next section, and those obtained from separate teleseismic tomography studies using LF98 (Graeber et al., 2002), SEAL (Rawlinson and Urvoy, 2006) and EVA (Rawlinson and Kennett, 2008), shows that they are consistent, with the only real differences occurring near the edges of the arrays.

Fig. 8 shows long wavelength (~200 km and upwards) variations in S-wave velocity obtained from surface wave tomography (Fishwick et al., 2008) at 150 km depth. The main trend is a W–E decrease in shear velocity from about 4.4 km/s to 4.2 km/s, although further north, it is oriented more in the ESE direction, with velocities as high as 4.6 km/s in the northwest corner of the plot. Assuming that variations in P-wavespeed exhibit a similar pattern, then this would reflect the background velocity trend that is likely to be filtered out by the joint inversion of residuals.

Instead of using relative arrival times to image structure beneath WOMBAT, an alternative approach is to use absolute times, which would mitigate the potential issues described previously. This has been done using USArray (e.g. Burdick et al., 2008), but requires the local model to be embedded within a global model in order to account for structure outside the region of interest. Invariably this involves the use of sophisticated adaptive gridding techniques to allow for a wide range of resolvable scale lengths. Also, the potentially large errors in origin time may result in some loss of detail of fine scale structure. A more robust approach may be to generate a broad scale velocity model using the absolute times, and then invert for small scale velocity variations using precise relative arrival times.

3.3. Tomographic model

The inversion procedure used to obtain the final model from the joint datasets of WOMBAT is exactly the same as that used for the checkerboard test described above (see Figs. 5–7). Six iterations of the tomographic scheme are used to reduce the RMS traveltime residuals from 244 ms to 143 ms, which corresponds to a variance reduction of 61%. While it is possible to reduce the RMS residual to below 130 ms by decreasing the value of the smoothing parameter, we favour a less detailed model in order to avoid over-interpretation. A series of horizontal and vertical sections through the solution model are shown in Figs. 9 and 10 respectively. Perhaps the largest change in lateral structure with depth occurs between 50 and 100 km depth (cf. Fig. 9a and b); this is not particularly surprising since at 50 km depth, we are just below the base of the Moho, where there is potential for shallow crustal structure to smear into uppermost mantle structure.

The dominant direction of structural variation in Fig. 9 is clearly in the E–W direction at depths below 100 km, and according to the checkerboard resolution tests of Figs. 5 and 6, this is well constrained to the base of the model. So also are a number of smaller scale features including the elevated velocity zone in the vicinity of the Melbourne Zone at depths of 100 km and greater. Its absence in the 50 km depth section (Fig. 9a) may be due to the masking effects of unresolved near-surface structure. In general, velocity anomalies do not tend to exceed ±2.5% (±0.2 km/s), although these bounds are strongly dependent on the choice of smoothing and damping regularisation.

In interpreting Figs. 9 and 10, it must be remembered that longer wavelength velocity features are absent. Thus, the absolute values of the velocity perturbations in one area of the model may not be directly comparable to those in another, particularly if it is beneath a different array. For instance, the positive velocity anomaly at about 147° longitude in Fig. 9c does not imply that the absolute velocity in this location is higher than at, say, 139° longitude (beneath the mainland), where there is a pronounced negative anomaly. Inspection of Fig. 8 shows a generally easterly decrease in absolute velocity across the model (which is presumably similar for P-waves), implying that, in absolute terms, the situation is likely reversed. Although this kind of observation complicates interpretation somewhat, features such as localised velocity gradients – which are suggestive of boundaries – can still be interpreted in a relatively straight forward manner.

4. Discussion

The model obtained by joint inversion of WOMBAT teleseismic arrival time residuals (Figs. 9 and 10) reveals a variety of anomalies, but for the purposes of this study, we concentrate on the longer wavelength features (greater than ~100 km), even though structures as small as 50 km across can be resolved in some areas. Fig. 9 clearly

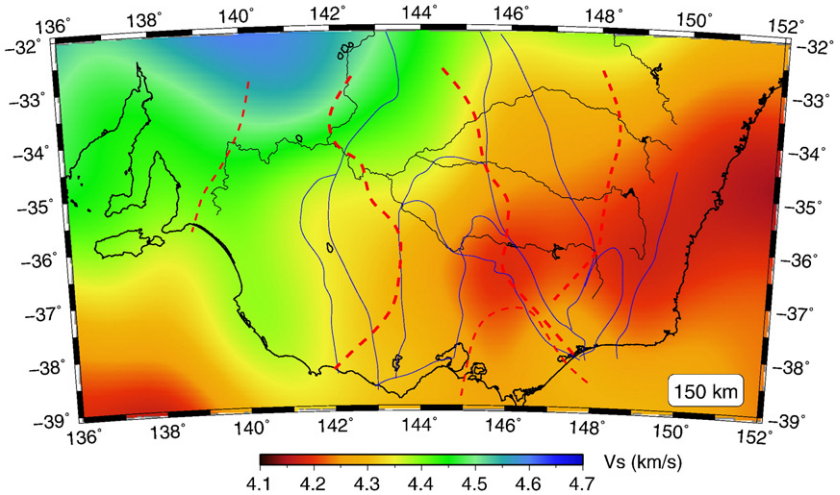

Fig. 8. Broad scale shear wavespeed variations at 150 km depth obtained from surface wave tomography. Major Palaeozoic boundaries from Fig. 1 have been superimposed, together with the zone boundaries defined in Fig. 11b.

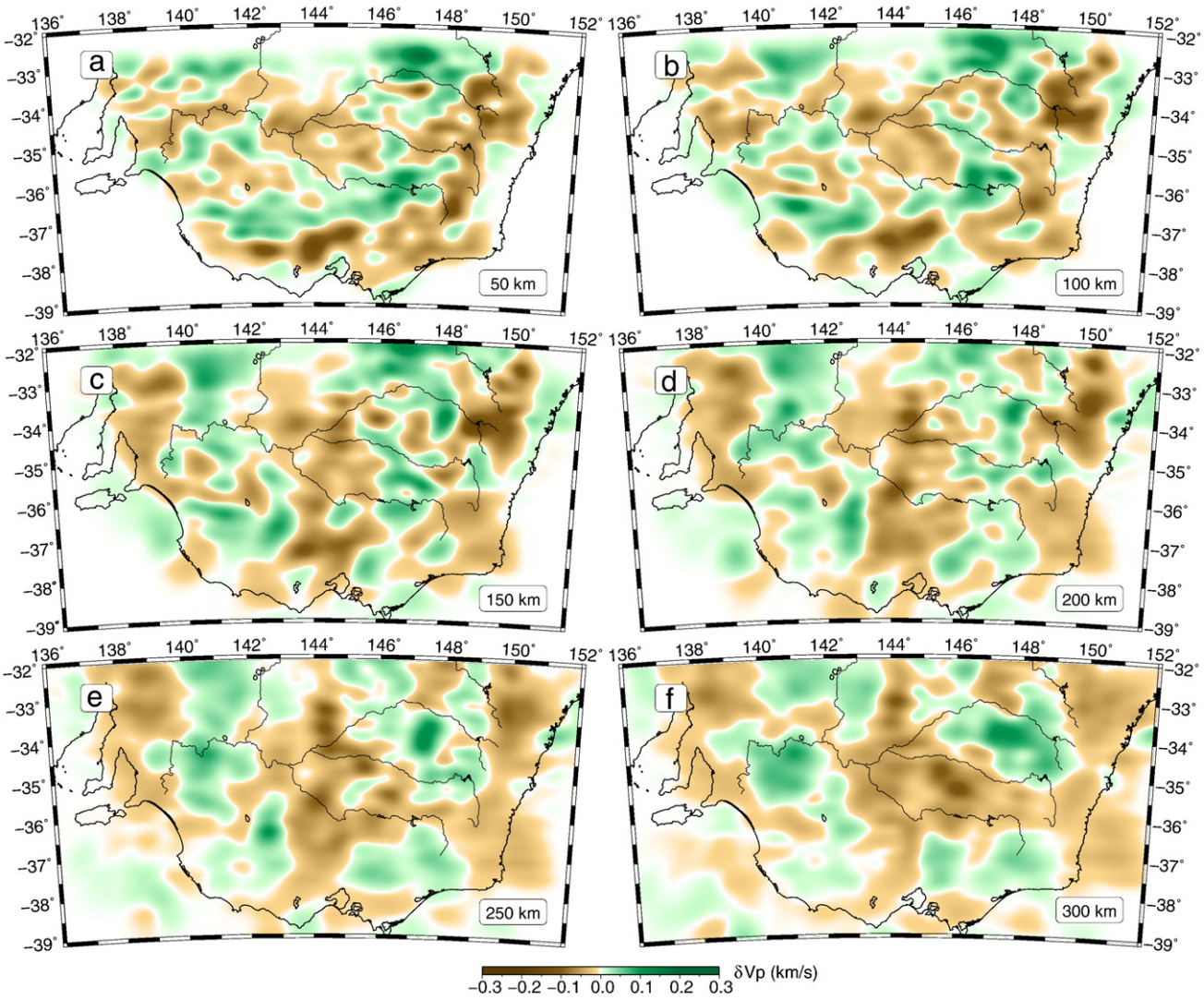

Fig. 9. Horizontal slices through the 3-D velocity model obtained by inversion of WOMBAT teleseismic arrival time residuals.

illustrates that the first-order pattern of velocity anomalies changes from predominantly E–W striking features at 50 km depth to largely N–S striking features at 150 km depth. To help facilitate interpretation, two depth slices – one near the top of the mantle lithosphere and one near the bottom of the mantle lithosphere – are shown in Fig. 11 with significant features highlighted. One of the challenges in attempting to interpret these images is the difficulty in trying to separate the signatures of Palaeozoic lithospheric evolution associated with the formation of the Delamerian and Lachlan Orogens, and more recent tectonic events such as the Mesozoic rifting of Australia and Antarctica, which likely affected structures inboard of the margin (Foster and Gleadow, 1992).

The 50 km depth slice (Fig. 11a) reveals a pattern of velocity variations that bears little resemblance to the Palaeozoic boundaries plotted in Fig. 1. If these boundaries actually represent major divisions between crustal blocks of different character, then one might expect them to continue into the lithosphere and hence manifest in images of seismic velocity. The fact that they do not may mean that these boundaries are limited to the crust – or even upper crust – which is quite possible since they are largely inferred from surface geology and potential field data. Another possibility is that the changes in properties in the lithosphere are not sufficient to give rise to a change in seismic velocity, even though boundaries are present. A third possibility is that more recent effects, which post-date the Palaeozoic orogenies, have strongly influenced the seismic properties of this region of the lithosphere. For instance, the break-up of Australia and Antarctica, which began at ~160 Ma, resulted in the formation of the Mesozoic–Cainozoic Bass Basin (Fig. 1), a failed intra-cratonic rift basin (Gunn et al., 1997), which separates Victoria and Tasmania. Passive continental margins can evolve in a variety of ways (Lister et al., 1986, 1991), but one possibility is for lithospheric scale detachment faults to produce asymmetric margins. The lower plate side is underpinned by stretched mantle lithosphere, whereas the upper plate side has the mantle lithosphere removed, and is directly exposed to the asthenosphere. This can result in basaltic underplating beneath the crust (Lister et al., 1986). Furthermore, it is possible for the fault beneath the upper plate side to propagate horizontally for some distance, so that the underplating zone occurs at a significant distance from the onset of oceanic lithosphere. This effect may explain the high velocity zone observed in Fig. 11a.

Another important consideration is the Newer Volcanic Provinces in Victoria (see Fig. 1), which was mentioned earlier. It is quite likely that the elevated temperatures associated with recent hot-spot volcanism (4.5 Ma to <10 ka, see Price et al., 1997) has resulted in the pronounced negative velocity perturbation highlighted in Fig. 11a. Finally, it is also worth noting that 50 km represents the minimum depth of resolution, and lies in the vicinity of the Moho. While it is hoped that the inclusion of station terms in the inversion removed

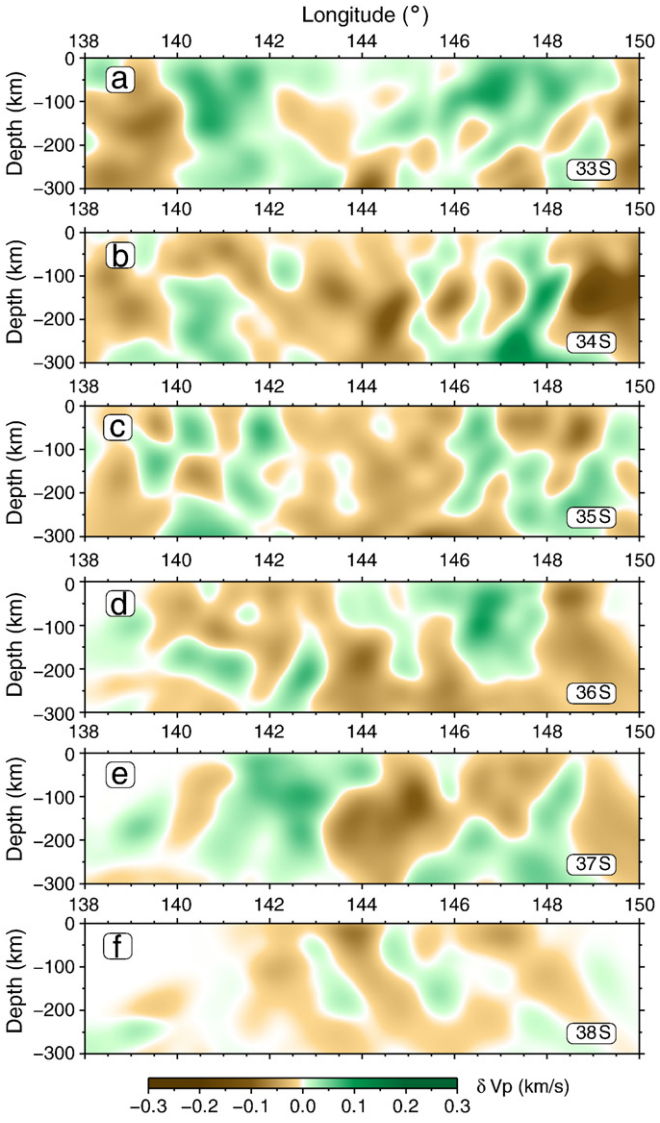

Fig. 10. E–W cross-sections through the 3-D velocity model obtained by inversion of WOMBAT teleseismic arrival time residuals. The ratio between the vertical and horizontal scale is unity (i.e. no vertical exaggeration).

unresolved crustal effects from the final model, it is quite likely that crustal artefacts are present at this depth. In particular, the crustal root of the Great Dividing Range, which runs down the east coast of southeast Australia and terminates in eastern Victoria (Fig. 2), probably contributes to the lower velocities observed inboard of the east and southeast coastlines (Fig. 11a). That said, it is interesting to note that in a recent ambient noise tomography study of the same region using data from WOMBAT (Arroucau et al., 2010), no clear evidence of Palaeozoic boundaries was detected in Rayleigh wave group velocity images of the crust.

If we now inspect the 150 km slice (Fig. 11b), a broad W–E trend of velocity variations is readily observed which contrasts significantly with the patterns observed in the 50 km slice, particularly in the south. Five broad zones have been identified, which may represent lithosphere of different character. One of the main targets of WOMBAT in southeast Australia is the location and nature of the transition between the Delamerian and Lachlan orogens at upper mantle depths. As Fig. 11 shows, there is significant change from higher to lower velocity between Zones 2 and 3, which may reflect the eastern edge of the Delamerian Orogen. If this is the case, then the Delamerian Orogen underlies much of the Stawell Zone and hence the western edge of the Lachlan Orogen. The change from higher wavespeeds in the west to lower wavespeeds in the east is consistent with a change from Proterozoic mantle lithosphere of continental origin to Phanerozoic mantle lithosphere of oceanic origin; expected changes in both composition (Griffin et al., 1998; Cammarano et al., 2003) and temperature (Faul and Jackson, 2005) between these two types of material make this a plausible proposition. Furthermore, this boundary has also been observed as an eastward change from higher to lower shear wavespeed, albeit at much lower resolution using surface wave tomography (Simons et al., 2002; Fishwick et al., 2008), which appears to discriminate between cratonic western/central Australia and the accretionary orogens to the east. Regional and global tomography studies generally reveal a positive correlation between lithospheric age, thickness and seismic wavespeed (Simons et al., 2002), the implication being that older thicker lithosphere is cooler and exhibits higher seismic wavespeeds compared to younger, thinner and hotter lithosphere. However, as noted by Simons and van der Hilst, 2002, this correlation can break down due to variations in composition and mechanical strength.

Before continuing, it is worth introducing several caveats. First, the Newer Volcanic Provinces and possible magmatic underplating and stretching of the lithosphere associated with the Bass and Otway basins and the Tasman Sea may have significantly altered the character of the lithosphere at 150 km depth. For instance, the southerly extent of Zone 3 may be enhanced by the thermal signatures of these events. Furthermore, if significant detachment faulting and underplating did occur, as suggested in the 50 km slice, would the lithosphere still contain clear and continuous remnants of Palaeozoic structure at greater depth? Currently, there is insufficient information to properly answer this question, but the clear emergence of distinct zones at 150 km depth could be used to argue that the slices at shallow depth are heavily influenced by the effects of near-surface structure, which is only properly removed at 100 km depth and beyond. A second caveat is that at 150 km, it could be argued that the velocity perturbations reflect structure at the very base of the lithosphere, or even in the sub-lithospheric mantle. In eastern Australia, the lithosphere is likely to be markedly thinner compared to western and central Australia, where the lithospheric keel beneath Archean cratons can extend to 250 km depth or more (Simons and van der Hilst, 2002). One possibility is that the velocity variation observed between Zones 2 and 3 represents the difference between a mechanically strong lithosphere in the west, and weaker (and hence slower) sub-lithospheric mantle in the east. However, even if this interpretation is correct, it does not undermine the possibility that the transition between Zone 2 and 3 reflects the boundary between the Delamerian and Lachlan Orogens. In this case, however, the demarcation would be between thicker and thinner lithosphere, rather than faster and slower lithosphere. Finally, it is also worth noting that teleseismic tomography has a propensity to smear structure in the vertical direction (see Fig. 6), so velocity variations observed at 150 km depth may reflect shallower structures in the lithosphere.

With regard to earlier discussion on the nature of the Delamerian–Lachlan boundary, the upper mantle location of the velocity transition is consistent with an easterly dipping Moyston Fault (Korsch et al., 2002), the surface trace of which lies to the west of the boundary inferred in Fig. 11b. An alternative interpretation is that the elevated velocities beneath the Stawell Zone signal the presence of a Proterozoic continental fragment, as inferred by Miller et al. (2005). While this may be possible, it should be noted that they position the eastern edge of this fragment along the Moyston Fault. In cross-section view (Fig. 10), the boundary between higher and lower wavespeeds is not very distinct, which may be due in part to the overprinting effects referred to above, and the potential blurring of the boundary by the presence of a reworked orogenic zone (Miller et al., 2005). Fig. 9c–f do imply that the inferred Delamerian–Lachlan velocity boundary in the upper mantle is nearly

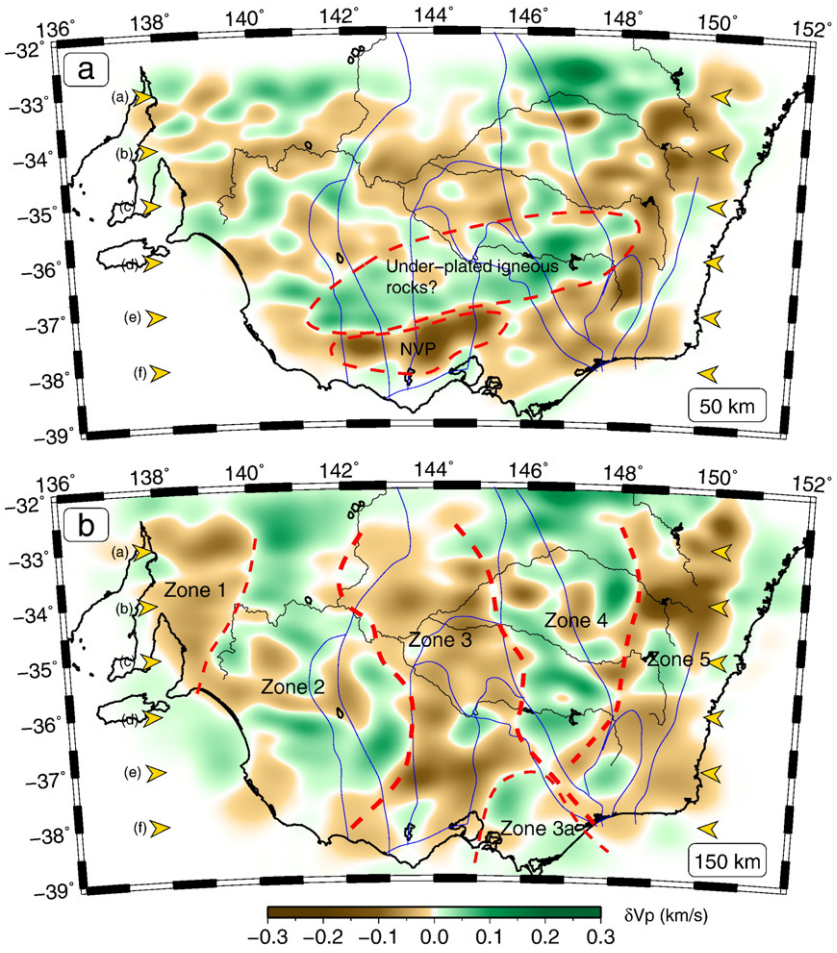

Fig. 11. Horizontal section through the solution model at (a) 50 km depth, and (b) 150 km depth with several significant features highlighted. Major Palaeozoic boundaries from Fig. 1 have also been superimposed for reference. Yellow arrows denote the locations of E–W cross-sections shown in Fig. 10.

vertical, which is consistent with inferences made from Nd and Os isotope data in the vicinity of the Moyston Fault (Handler and Bennet, 2001; Korsch et al., 2002).

Another N–S trending feature in the model is an easterly transition from lower velocities in Zone 3 to higher velocities in Zone 4. This may represent the change from the Western to the Central Subprovince of the Lachlan Orogen at depth. The Central Subprovince largely incorporates the Omeo Zone, which extends into New South Wales where it becomes the Wagga Zone (although there is no defined boundary between the two), and represents the main concentration of Palaeozoic intermediate-to-high-grade, low pressure metamorphism in the Lachlan Orogen (Foster and Gray, 2000). There are several possible explanations for the presence of this boundary, including eastward subduction of oceanic lithosphere beneath an island-arc complex to form a high-temperature metamorphic/plutonic zone, followed by double-divergent subduction (Foster and Gray, 2000; Spaggiari et al., 2003). Remnant underplated oceanic lithosphere may well produce such a velocity contrast. An alternative explanation is that the elevated velocities are associated with the presence of a Proterozoic continental fragment or ribbon detached from the supercontinent Rodinia and subsequently trapped within the accretionary melange of the Lachlan Orogen, as suggested by Rawlinson and Kennett (2008). The potential for fragments of Rodinia to be incorporated in the Tasman Orogen has been recognised by a variety of authors in the past (e.g. Glen et al., 1992; Cayley et al., 2002; Betts et al., 2002; Gray and Foster, 2004; Glen, 2005).

In their 2002 paper, Cayley et al. (2002) present a case for the existence of a Proterozoic continental fragment beneath the Melbourne Zone, which they call the "Selwyn Block" (see also Scheibner and Veevers, 2000). On the basis of aeromagnetic and geological data, the former of which shows evidence for continuous structures beneath Bass Strait that link mainland Australia to Proterozoic western Tasmania, it is argued that a large continental fragment lies beneath this region of Australia. Recent work from reflection seismic transects in central and western Victoria has provided additional support for this model (Cayley et al., in press). In Fig. 11b, Zone 3a outlines the high velocity anomaly that lies beneath the Melbourne Zone in Victoria. This anomaly is extensive in depth, and may well reflect the presence of a Proterozoic continental fragment. However, resolution in the far south of the model is limited due to the lack of earthquakes from the south, so this feature is not well constrained. Moreover, the overprinting effects of the Newer Volcanic Provinces may have limited the westerly extent of Zone 3a. Nonetheless, it does provide some support to the Selwyn Block idea, and if the Omeo Zone is indeed underlain by a continental fragment, then it may well be that a very extensive ribbon of Proterozoic material extends from Tasmania northward into New South Wales.

Other features of the solution model that have been highlighted include a marked velocity contrast between Zones 4 and 5 which may be associated with the change from the Central to the Eastern Subprovince of the Lachlan Orogen. This occurs some distance eastward of the change near the surface (see Fig. 1). However, we are more cautious of our interpretation in this region of the model, due to possible overprinting effects from recent volcanism under the southeast Lachlan near the east coast of Australia, and evidence from surface wave tomography that the lithosphere becomes quite thin

towards the eastern coastline (Fishwick et al., 2008). In the far west of the model (Fig. 11b), there is a low velocity region that may be a signature of the Adelaide rift complex, the eastern edge of which marks the beginning of the Delamerian Orogen. Again, we emphasise that this negative anomaly is only negative relative to the adjoining velocities to the east, and does not automatically imply low velocities relative to, say, those beneath Zone 4 (see Fig. 8).

Future work includes incorporating additional teleseismic data from recent deployments of WOMBAT in central New South Wales and southern South Australia as they become available; using absolute arrival time information to constrain broad scale variations in wavespeed; and including information from ambient noise surface wave tomography, which provide valuable constraints on crustal structure that is not resolved by teleseismic data. Additional constraints on mantle velocities are required to properly explain the relationship between features observed near the top and bottom of the mantle lithosphere.

5. Conclusions

In this study, teleseismic data from seven sub-arrays of the WOMBAT rolling array project in southeast Australia are simultaneously inverted to produce a new and detailed 3-D model of P-wave velocity perturbations in the upper mantle. The imaging results reveal a variety of distinct features in the lithospheric mantle which reflect the complex evolution history of this region of the Australian plate. At shallow depths (~50 km), the recovered pattern of velocity anomalies tends to strike E–W, and shares little resemblance to observed and inferred terrane boundaries in the shallow crust. A large region of elevated velocity that spans much of Victoria may be related to basaltic underplating associated with the formation of the Bass Basin during the separation of Australia and Antarctica. Distinct negative velocity perturbations to the north and east of Melbourne appear to correlate well with the location of the Quaternary Newer Volcanic Provinces. Towards the base of the lithosphere (~150 km), the pattern of velocity perturbations has a predominantly N–S strike, and five distinct velocity zones have been identified. A clear easterly transition from higher to lower velocities beneath the Stawell Zone may represent the transition from the Delamerian (Proterozoic continentally derived lithosphere) to the Lachlan (Palaeozoic oceanic derived lithosphere) Orogen at depth. Further east, elevated velocities beneath the Omeo Zone may indicate that the Central Subprovince of the Lachlan Orogen is underlain by a large Proterozoic continental fragment derived from the Neoproterozoic break-up of Rodinia.

Acknowledgments

This work is supported by ARC Discovery Project DP0986750. Anya Reading and an anonymous reviewer are thanked for their constructive comments on the original version of the manuscript.

References

Aki, K., Christoffersson, A., Husebye, E.S., 1977. Determination of the three-dimensional seismic structure of the lithosphere. Journal of Geophysical Research. 82, 277–296.
Arroucau, P., Rawlinson, N., Sambridge, M., 2010. New insight into Cainozoic sedimentary basins and Palaeozoic suture zones in southeast Australia from ambient noise surface wave tomography. Geophysical Research Letters 37, L07303. doi:10.1029/2009GL041974.
Baillie, P.W., 1985. A Palaeozoic suture in eastern Gondwanaland. Tectonics 4, 653–660.
Berry, R.F., Steele, D.A., Meffre, S., 2008. Proterozoic metamorphism in Tasmania: implications for tectonic reconstructions. Precambrian Research 166, 387–396.
Betts, P.G., Giles, D., Lister, G.S., Frick, L., 2002. Evolution of the Australian lithosphere. Australian Journal of Earth Sciences 49, 661–695.
Burdick, S., Li, C., Martynov, V., Cox, T., Eakins, J., Astiz, L., Vernon, F.L., Pavlis, G.L., Van der Hilst, R.D., 2008. Upper mantle heterogeneity beneath North America from travel time tomography with global and USArray transportable array data. Seismological Research Letters 79, 384–392.
Cammarano, F., Goes, S., Vacher, P., Giardini, D., 2003. Inferring upper-mantle temperatures from seismic velocities. Physics of the Earth and Planetary Interiors 138, 197–222.
Cayley, R.A., Taylor, D.H., 1998. The Lachlan margin Victoria: the Moyston Fault, a newly recognised terrane boundary. Geological Society of Australia Abstracts 49, 73.
Cayley, R., Taylor, D.H., VandenBerg, A.H.M., Moore, D.H., 2002. Proterozoic–Early Palaeozoic rocks and the Tyennan Orogeny in central Victoria: the Selwyn Block and its tectonic implications. Australian Journal of Earth Sciences 49, 225–254.
Cayley, R., Korsch, R.J., Moore, D.H., Costello, R.D., Nakamura, A., Willman, C.E., Rawling, T.J., Morand, V.J., Skladzien, P.B., O'Shea, P.J., in press. Crustal architecture of central Victoria: results from the 2006 deep crustal reflection seismic survey. Australian Journal of Earth Sciences.
Clifford, P., Greenhalgh, S., Houseman, G., Graeber, F., 2008. 3-D seismic tomography of the Adelaide fold belt. Geophysical Journal International 172, 167–186.
Collins, C.D.N., 1991. The nature of the crust–mantle boundary under Australia from seismic evidence. In: Drummond, B. (Ed.), The Australian Lithosphere. : Special Publication, vol.17. Geological Society of Australia, pp. 67–80.
Direen, N.G., Crawford, A.J., 2003. The Tasman Line: where is it, what is it, and is it Australia's Rodinian breakup boundary? Australian Journal of Earth Sciences 50, 491–502.
Faul, U.H., Jackson, I., 2005. The seismological signature of temperature and grain size variations in the upper mantle. Earth and Planetary Science Letters 234, 119–134.
Fishwick, S., Heintz, M., Kennett, B.L.N., Reading, A.M., Yoshizawa, K., 2008. Steps in lithospheric thickness within eastern Australia, evidence from surface wave tomography. Tectonics 27. doi:10.1029/2007TC002116.
Foden, J., Elburg, M.A., Dougherty-Page, J., Burtt, A., 2006. The timing and duration of the Delamerian Orogeny: correlation with the Ross Orogen and implications for Gondwana assembly. Journal of Geology 114, 189–210.
Foster, D.A., Gleadow, A.J.W., 1992. Reactivated tectonic boundaries and implications for the reconstruction of south-eastern Australia and Northern Victoria land. Antarctica Geology 20, 267–270.
Foster, D.A., Gray, D.R., 2000. Evolution and structure of the Lachlan Fold Belt (Orogen) of eastern Australia. Annual Review of Earth and Planetary Sciences 28, 47–80.
Foster, D.A., Gray, D.R., Spaggiari, C., Kamenov, G., Bierlein, F.P., 2009. Palaeozoic Lachlan orogen, Australia; accretion and construction of continental crust in a marginal ocean setting: isotopic evidence from Cambrian metavolcanic rocks. Geological Society, London, Special Publications 318, 329–349.
Frederiksen, A.W., Bostock, M.G., VanDecar, J.C., Cassidy, J.F., 1998. Seismic structure of the upper mantle beneath the northern Canadian Cordillera from teleseismic travel-time inversion. Tectonophysics 294, 43–55.
Glahn, A., Granet, M., 1993. Southern Rhine Graben: small-wavelength tomographic study and implications for the dynamic evolution of the graben. Geophysical Journal International 113, 399–418.
Glen, R.A., 2005. The Tasmanides of eastern Australia. In: Vaughan, A.P.M., Leat, P.T., Pankhurst, R.J. (Eds.), Terrane Processes at the Margins of Gondwana. Geological Society, London, pp. 23–96.
Glen, R.A., Scheibner, E., Vandenberg, A.H.M., 1992. Paleozoic intraplate escape tectonics in Gondwanaland and major strike-slip duplication in the Lachlan Orogen of south-eastern Australia. Geology 20, 795–798.
Glen, R.A., Percival, I.G., Quinn, C.D., 2009. Ordovician continental margin terranes in the Lachlan Orogen, Australia: implications for tectonics in an accretionary orogen along the east Gondwana margin. Tectonics 28. doi:10.1029/2009TC002446.
Graeber, F.M., Asch, G., 1999. Three-dimensional models of *P* wave velocity and *P*-to-*S* velocity ratio in the southern central Andes by simultaneous inversion of local earthquake data. Journal of Geophysical Research 104, 20,237–20,256.
Graeber, F.M., Houseman, G.A., Greenhalgh, S.A., 2002. Regional teleseismic tomography of the western Lachlan Orogen and the Newer Volcanic Province, southeast Australia. Geophysical Journal International 149, 249–266.
Gray, D.R., Foster, D.A., 2004. Tectonic evolution of the Lachlan Orogen, southeast Australia: historical review, data synthesis and modern perspectives. Australian Journal of Earth Sciences 51, 773–817.
Griffin, W.L., O'Reilly, S.Y., Ryan, C.G., Gaul, O., Ionov, D.A., 1998. Secular variation in the composition of subcontinental lithospheric mantle: geophysical and geodynamic implications. In: Braun, J., Dooley, J., Goleby, B., van der Hilst, R., Klootwijk, C. (Eds.), Structure and Evolution of the Australian Continent: American Geophysical Union Geodynamic Series, vol.26, pp. 1–26.
Gunn, P.J., Mitchell, J., Meixner, A., 1997. The structure and evolution of the bass basin as delineated by aeromagnetic data. Exploration Geophysics 28, 214–219.
Handler, M.R., Bennet, V.C., 2001. Constraining continental structure by integrating Os isotopic ages of lithospheric mantle with geophysical and crustal data: an example from southeastern Australia. Tectonics 20, 177–188.
Hearn, T.M., Clayton, R.W., 1986. Lateral velocity variations in southern California. I. Results for the upper crust from Pg waves. Bulletin of the Seismological Society of America 76, 495–509.
Humphreys, E.D., Clayton, R.W., 1990. Tomographic image of the Southern California Mantle. Journal of Geophysical Research 95, 19,725–19,746.
Kennett, B.L.N., Sambridge, M.S., Williamson, P.R., 1988. Subspace methods for large scale inverse problems involving multiple parameter classes. Geophysical Journal 94, 237–247.
Kennett, B.L.N., Engdahl, E.R., Buland, R., 1995. Constraints on seismic velocities in the earth from travel times. Geophysical Journal International 122, 108–124.
Korsch, R.J., Barton, T.J., Gray, D.R., Owen, A.J., Foster, D.A., 2002. Geological interpretation of a deep seismic-reflection transect across the boundary between the Delamerian and Lachlan Orogens, in the vicinity of the Grampians, western Victoria. Australian Journal of Earth Sciences 49, 1057–1075.

Lei, J., Zhao, D., 2007. Teleseismic P-wave tomography and the upper mantle structure of the central Tien Shan orogenic belt. Physics of the Earth and Planetary Interiors 162, 165–185.
Lévêque, J.J., Rivera, L., Wittlinger, G., 1993. On the use of the checker-board test to assess the resolution of tomographic inversions. Geophysical Journal International 115, 313–318.
Lippitsch, R., Kissling, E., Ansorge, J., 2003. Upper mantle structure beneath the Alpine orogen from high-resolution teleseismic tomography. Journal of Geophysical Research 108, 2376. doi:10.1029/2002JB002016.
Lister, G.S., Ethridge, M.A., Symonds, P.A., 1986. Detachment faulting and the evolution of passive continental margins. Geology 14, 246–250.
Lister, G.S., Ethridge, M.A., Symonds, P.A., 1991. Detachment models for the formation of passive continental margins. Tectonics 10, 1038–1064.
Martin, M., Ritter, J.R.R., the CALIXTO working group, 2005. High-resolution teleseismic body-wave tomography beneath SE Romania — I. Implications for the three-dimensional versus one-dimensional crustal correction strategies with a new crustal velocity model. Geophysical Journal International 162, 448–460.
Menke, W., 1989. Geophysical Data Analysis: Discrete Inverse Theory. Academic Press, New York.
Miller, J.M., Phillips, D., Wilson, C.J.L., Dugdale, L.J., 2005. Evolution of a reworked orogenic zone: the boundary between the Delamerian and Lachlan fold belts, southeastern Australia. Australian Journal of Earth Sciences 52, 921–940.
Popovici, A.M., Sethian, J.A., 2002. 3-D imaging using higher order fast marching traveltimes. Geophysics 67, 604–609.
Price, R.C., Gray, C.M., Frey, F.A., 1997. Strontium isotopic and trace element heterogeneity in the plains basalts of the Newer Volcanic Province, Victoria, Australia. Geochimica et Cosmochimica Acta 61, 171–192.
Priestley, K., Tilmann, F., 2009. Relationship between the upper mantle high velocity seismic lid and the continental lithosphere. Lithos 109, 112–124.
Rawlinson, N., Kennett, B.L.N., 2004. Rapid estimation of relative and absolute delay times across a network by adaptive stacking. Geophysical Journal International 157, 332–340.
Rawlinson, N., Kennett, B.L.N., 2008. Teleseismic tomography of the upper mantle beneath the southern Lachan Orogen, Australia. Physics of the Earth and Planetary Interiors 167, 84–97.
Rawlinson, N., Sambridge, M., 2003. Seismic traveltime tomography of the crust and lithosphere. Advances in Geophysics 46, 81–198.
Rawlinson, N., Sambridge, M., 2004a. Multiple reflection and transmission phases in complex layered media using a multistage fast marching method. Geophysics 69, 1338–1350.
Rawlinson, N., Sambridge, M., 2004b. Wavefront evolution in strongly heterogeneous layered media using the fast marching method. Geophysical Journal International 156, 631–647.
Rawlinson, N., Urvoy, M., 2006. Simultaneous inversion of active and passive source datasets for 3-D seismic structure with application to Tasmania. Geophysical Research Letters 33. doi:10.1029/2006GL028105.
Rawlinson, N., Kennett, B.L.N., Heintz, M., 2006a. Insights into the structure of the upper mantle beneath the Murray Basin from 3D teleseismic tomography. Australian Journal of Earth Sciences 53, 595–604.
Rawlinson, N., Reading, A.M., Kennett, B.L.N., 2006b. Lithospheric structure of Tasmania from a novel form of teleseismic tomography. Journal of Geophysical Research 111. doi:10.1029/2005JB003803.
Rawlinson, N., Pozgay, S., Fishwick, S., 2010. Seismic tomography: a window into deep Earth. Physics of the Earth and Planetary Interiors 178, 101–135.
Rutland, R.W.R., 1976. Orogenic evolution of Australia. Earth Science Reviews 12, 161–196.
Scheibner, E., Veevers, J.J., 2000. Tasman Fold Belt System. In: Veevers, J.J. (Ed.), Billion-Year Earth History of Australia and Neighbours in Gondwanaland. Sydney, GEMOC Press, Macquarie Univ., pp. 154–234.
Simons, F.J., van der Hilst, R.D., 2002. Age-dependent seismic thickness and mechanical strength of the australian lithosphere. Geophysical Research Letters 29. doi:10.1029/2002GL014962.
Simons, F.J., van der Hilst, R.D., Montagner, J.-P., Zielhuis, A., 2002. Multimode Rayleigh wave inversion for heterogeneity and azimuthal anisotropy of the Australian upper mantle. Geophysical Journal International 151, 738–754.
Spaggiari, C.V., Gray, D.R., Foster, D.A., McKnight, S., 2003. Evolution of the boundary between the western and central Lachlan Orogen: implications for Tasmanide tectonics. Australian Journal of Earth Sciences 50, 725–749.
Spaggiari, C.V., Gray, D.R., Foster, D.A., 2004. Lachlan Orogen subduction–accretion systematics revisited. Australian Journal of Earth Sciences 51, 549–553.
Taylor, D.H., Cayley, R.A., 2000. Character and kinematics of faults within the turbidite-dominated Lachlan Orogen: implications for tectonic evolution of eastern Australia: discussion. Journal of Structural Geology 22, 523–528.
VandenBerg, A.H.M., 1978. The Tasman fold belt system in Victoria. Tectonophysics 48, 267–297.
VandenBerg, A.H.M., 1999. Timing of orogenic events in the Lachlan Orogen. Australian Journal of Earth Sciences 46, 691–701.
Waldhauser, F., Lippitsch, R., Kissling, E., Ansorge, J., 2002. High-resolution teleseismic tomography of upper-mantle structure using an *a priori* three-dimensional crustal model. Geophysical Journal International 150, 403–414.
Willman, C.E., VandenBerg, A.H.M., Morand, V.J., 2002. Evolution of the southeastern Lachlan Fold Belt in Victoria. Australian Journal of Earth Sciences 49, 271–289.